Molecular Vision 2020; 26:494-504 <http://www.molvis.org/molvis/v26/494>
Received 31 October 2019 | Accepted 25 June 2020 | Published 27 June 2020

Tetramethylpyrazine protects mice retinas against sodium iodate–induced oxidative injury

Jie Huang,[1,2] Yan Liu,[1] Ke Mao,[1] Qing Gu,[1] Xingwei Wu[1]

[1]Department of Ophthalmology, Shanghai General Hospital of Nanjing Medical University, Shanghai, China; [2]Department of Ophthalmology, Baoshan Hospital of Integrated Traditional Chinese Medicine and Western Medicine, Shanghai, China

Purpose: To observe the effects of tetramethylpyrazine (TMP) on mice retinas injured by sodium iodate ($NaIO_3$).
Methods: Male mice (n = 45) were randomly divided into three groups: the control group (Group C), the $NaIO_3$-degenerated group (Group I), and the TMP-treated group (TMP group). The Group I mice were intraperitoneally injected with 35 mg/kg $NaIO_3$. The Group C mice were injected with similar volumes of PBS. The TMP group mice were intraperitoneally injected with 80 mg/kg TMP starting 24 h after $NaIO_3$ administration once a day for 14 days. Fundus photography, optical coherence tomography (OCT), electroretinography (ERG), hematoxylin and eosin (H&E) staining, terminal deoxynucleotidyl transferase dUTP nick-end labeling (TUNEL) assay, and western blotting were used to assess the effects of TMP on mice retinas at day 3, 7, and 14 after $NaIO_3$ administration.
Results: TMP effectively prevented the decrease in the thicknesses of the retinas and the outer nuclear layer (ONL), and effectively alleviated the functional decline in the retinas after $NaIO_3$ administration. TMP significantly decreased the number of TUNEL-positive cells in retinas. In addition, TMP rapidly increased the expression of Nrf2 and HO-1 and decreased BAX expression in mice retinas after $NaIO_3$ injection.
Conclusions: TMP alleviates morphological and functional retinal damage in mice exposed to $NaIO_3$ and reduces retinal apoptosis.

Age-related macular degeneration (AMD) is the leading cause of irreversible blindness in individuals over 65 years old in developed countries [1]. AMD is characterized by the progressive loss of central vision and is classified into two forms: dry AMD and wet AMD. Dry AMD involves the accumulation of deposits in the RPE and Bruch's membrane and is characterized by drusen and geographic atrophy (GA). Wet AMD is characterized by choroidal neovascularization invading the RPE layer accompanied by bleeding and exudation. Both types eventually show degeneration of the RPE and photoreceptor cells. In recent years, anti-vascular endothelial factor (anti-VEGF) injections have revolutionized the treatment of wet AMD [2]. There are a few promising therapies under investigation, including stem cell transplantation [3]. For dry AMD, no definitive treatments are currently available.

Although the pathogenesis of AMD remains unclear, one of the risk factors is oxidative stress injury of the RPE [4]. Sodium iodate ($NaIO_3$), an oxidizing agent, effectively induces retinal degeneration associated with regional loss of RPE, recapitulating some of the morphological features of geographic atrophy [5]. $NaIO_3$ selectively injures the RPE with secondary effects on photoreceptors which makes it possible to establish a reproducible model of AMD [6,7]. $NaIO_3$–induced retinal structural and functional changes are time and dose dependent [8]. Treatment with >20 mg/kg $NaIO_3$ induces visual dysfunction associated with rapid suppression of phototransduction genes and induces oxidative stress in photoreceptors. $NaIO_3$ can directly alter photoreceptor function and survival [6]. Intravenous injection of 35 mg/kg $NaIO_3$ induces necrosis in RPE cells and apoptosis in photoreceptor cells [9].

Tetramethylpyrazine (TMP) is extracted from an active ingredient of traditional Chinese herbal medicine *Ligusticum wallichii* Franchat (Chuanxiong). It has been widely used for treatment of neurovascular disorders, such as ischemic stroke, in China for hundreds of years [10,11]. TMP efficiently protects retinal cells against hydrogen peroxide–induced oxidative stress in mixed rat retinal cell cultures [12]. In addition, TMP protects retinal capillary endothelial cells (TR-iBRB2) against IL-1β-induced nitrative and oxidative stress [13]. In recent years, TMP has been suggested for the treatment of various retinal diseases due to its antioxidant and anti-inflammatory effects.

In this study, we performed in vivo experiments to examine the protective effects of TMP on $NaIO_3$-induced retinal damage. Morphological and functional changes were assessed.

Correspondence to: Xingwei Wu, Department of Ophthalmology, Shanghai General Hospital of Nanjing Medical University, Shanghai, China Phone: +86-13918757688; email: wxweye@sina.com

METHODS

Animals: Forty-five 6- to 8-week-old male C57BL/6J mice (19–24 g) from Shanghai Laboratory Animal Center of the Chinese Academy of Sciences were randomly divided into three groups (the control group, Group C; the $NaIO_3$-degenerated group, Group I; and the TMP-treated group, TMP group), and housed in a standard laboratory environment under a 12-h:12-h light-dark cycle at 25 °C. All experimental procedures involving animals were performed in accordance with the ARVO Statement for the Use of Animals in Ophthalmic and Vision Research, and approved by the Institutional Animal Care and Use Committee of Shanghai General Hospital's Ophthalmic Research Center.

$NaIO_3$ and TMP Injection: A sterile 7 mg/ml $NaIO_3$ (S4007; Sigma St. Louis, MO) solution was freshly prepared with solid $NaIO_3$ diluted in PBS (1X; 120 mM NaCl, 20 mM KCl, 10 mM Na_2HPO_4, 5 mM KH_2PO_4, pH 7.4). Group I (the $NaIO_3$ group) was intraperitoneally injected with 35 mg/kg $NaIO_3$ solution. Group C (the control group) was injected with similar volumes of PBS. The TMP (95,162; Sigma) solution was freshly prepared as 10 mg/ml in dimethyl sulfoxide (DMSO): PBS 1/1,000 (v/v). The TMP group was intraperitoneally administered 80 mg/kg TMP solution beginning 24 h after treatment with 35 mg/kg $NaIO_3$ once a day for 14 days.

Optical coherence tomography and fundus photography: The mice were injected intraperitoneally with 4.3% chloral hydrate. Optical coherence tomography (OCT) images and fundus photography centered on the optic nerve head were acquired in live anesthetized animals using an OCT system (Phoenix Research Laboratories, Pleasanton, CA). Fundus images were obtained using the Micron III retinal imaging system in the same machine.

Electroretinography: Scotopic and photopic electroretinograms (ERGs) were recorded at day 3, 7, and 14 after $NaIO_3$ administration for four randomly selected mice (eight eyes) in each group. Following 6 h of dark adaptation, the mice were anesthetized with an intraperitoneal injection of 50 mg/kg ketamine plus 10 mg/kg xylazine and prepared under red light. The eyes were dilated with compound Tropicamide eye drops (SANTEN OY, Osaka, Japan). Ground and reference electrodes were placed subdermally on the tail and connected with the corneas, respectively. Scotopic and phototopic ERGs were collected on a Diagnosys Celeris instrument (Diagnosys, Boxborough, MA). Scotopic responses were elicited using eight flash intensities from 0.01 to 10 cd × s/m^2, with increasing interflash intervals at each step. Before the photopic ERG recordings, the mice were adapted to light via exposure to 5 min of bright white flashes (adapted with 30 cd × s/m^2 light). Photopic responses were elicited using a graded series of flashes with 3 cd × s/m^2 light, with the background presented on a 30 cd × s/m^2 background. All ERG data were collected at the same time of day. The a-wave amplitude was measured from the baseline to the trough of the first negative wave. The b-wave amplitude was measured from the trough of the a-wave to the peak of the first positive wave or from the baseline to the peak of the first positive wave in case of no a-wave.

Histology measurement: Whole eyes were enucleated, fixed with 10% formalin, paraffin embedded, and sectioned at 5 μm. The thicknesses of the retinas and the outer nuclear layer (ONL) of the retina's posterior pole were measured on hematoxylin and eosin (H&E)-stained slides. Five sections were measured for one eye of each mouse (one eye randomly selected from every mouse). The measurements were taken three times per section and averaged. For each section, measurements were taken at a distance of approximately 300 μm from the optic nerve.

TUNEL assay: The slides were washed with fresh xylene twice (15 min each time), rehydrated in a graded series of ethanol (absolute ethanol twice for 5 min, 85% and 75% ethanol each for 5 min), and rinsed in PBS for 5 min. The samples were then incubated in proteinase K for 15 min at room temperature and rinsed again three times in PBS for 5 min. The terminal deoxynucleotidyl transferase dUTP nick-end labeling (TUNEL) In situ Cell Death Detection Kit (Roche, Indianapolis, IN) was employed for the analysis according to the manufacturer's instructions. The slides were counterstained with 1 μg/ml 4′,6-diamidino-2-phenylindole (DAPI; Molecular Probes, Eugene, OR), incubated for another 10 min, rinsed in PBS three times for 5 min, and then sealed. A fluorescence scanning microscope (Olympus, Tokyo, Japan) was used for assessment.

Western blotting: Proteins were separated and transferred onto polyvinylidene fluoride (PVDF) membranes, which were incubated overnight at 4 °C with primary antibodies, including rabbit anti-mouse Nrf2 monoclonal antibodies (12,721; Cell Signaling Technology, Beverly, MA), rabbit anti-mouse HO-1 polyclonal antibodies (70,081; Cell Signaling Technology), rabbit anti-mouse Bax polyclonal antibodies (2772; Cell Signaling Technology), and rabbit anti-mouse β-actin monoclonal antibodies (4970; Cell Signaling Technology). Then, the membranes were incubated with horseradish peroxidase (HRP)-labeled anti-rabbit secondary antibodies (7047; Cell Signaling Technology) for 1 h at room temperature. The Chemi Doc XRS gel documentation system (Bio-Rad Laboratories Inc., Hercules, CA) was used to quantify immunoreactive proteins.

Statistical methods: Data were presented as mean ± standard error of the mean (SEM). A two-tailed *t* test was used for statistical analysis of two groups. To compare three groups, two-way analysis of variance (ANOVA) was used. All statistical analyses were performed using Graph Pad Prism 7.0 software (San Diego, CA). A p value of less than 0.05 was considered statistically significant .

RESULTS

Morphological changes in retinal tissue: To evaluate the effects of TMP in $NaIO_3$-induced injury in the mouse retinas, OCT and colorful fundus photographs of C57 mice in the three groups at day 3, 7, and 14 after administration of $NaIO_3$ were assessed (Figure 1). Three days after $NaIO_3$ treatment, the mouse retinas in Group I and the TMP group showed edemas (Figure 1B,C). Then the retinas were dark, and the pigments were disordered. Yellow-white deposits appeared at day 7 in Group I and the TMP group (Figure 1E,F). By day 14, the colors of the retinas were dirty, and the optic nerves were pale in the two groups (Figure 1H,I). OCT scans showed the retinal laminations in Group I and the TMP group became less clear compared with those in the control group at day 3 (Figure 2B,C). The RPE layers were disordered, and the RPE migrated into the inner and outer segments (IS/OS) at day 7 (Figure 2E,F). Progressive retinal degeneration was observed with RPE disruption and thinning of the entire retina, especially the ONL, in the following days. We could not identify laminations in Group I because of retinal atrophy at 14 days, and they were also blurry in the TMP group (Figure 2H,I).

Histological changes in the retinal tissue: H&E staining (Figure 3A) of the specimens confirmed the results from the fundus and OCT studies. The structure of each retinal layer in Group C was neatly arranged with an average thickness of 216 ± 3.00 μm; the ONL thickness was 49 ± 2.0 μm. After $NaIO_3$ treatment for 3 days, the ONLs in Group I and the TMP group were wave-like (Figure 3A); the normal RPE structure was destroyed, with swelling and bundling of RPE cells migrated. Black round sediments were observed in the IS/OS (Figure 3A). The entire retinas, especially the ONL, were thin in subsequent days in Group I and the TMP group, compared with Group C. The average retinal thicknesses in Group I were 147 ± 4 μm with an ONL thickness of 26 ± 2.0 μm; in the TMP group, values of 160 ± 5.00 μm and 25 ± 0.7 μm were obtained, respectively, for the retinal and ONL thicknesses. At day 7 after $NaIO_3$ injection, the thicknesses of the ONL were reduced more than 50%, with an average retinal thickness in Group I of 128 ± 4.00 μm, and an ONL thickness of 19 ± 5.0 μm. The average retinal and ONL thicknesses in the TMP group were 146 ± 13.0 μm and 25 ± 1.0 μm. On day 14, the average retinal thicknesses in Group I were 108 ± 4.00 μm, with an ONL thickness of 18 ± 3.0 μm. The average retinal and ONL thicknesses in the TMP group were 131 ± 6.00 μm and 26 ± 5.0 μm, respectively. The central retinal thicknesses of three groups statistically showed significant changes across time (**p<0.01). Retinal thicknesses reduction were less pronounced in the TMP group compared with Group I (**p<0.01; Figure 3B). ONL thicknesses of three groups also showed an apparent difference (**p<0.01), but they did not decrease statistically significantly across the time. The ONL thicknesses were reduced in Group I at day 7 and 14 compared with the TMP group (*p<0.05; Figure 3C). It appeared that TMP could prevent the decrease of the central retina and the ONL after $NaIO_3$ treatment.

ERG examinations in mice: Retinal function changes were examined with scotopic and photopic ERGs at day 3, 7, and 14 after $NaIO_3$ injection. Statistically significant reductions in all ERG responses were observed in Group I and the TMP group at three time points. The scotopic and photopic b-wave amplitudes strongly decreased from day 3 post $NaIO_3$ injection. In addition, visual function decreased by day 7, and the scotopic (b-wave) and photopic (b-wave) responses were almost diminished in Group I. These rapid ERG changes also appeared in the TMP group, but the reduction was less than in Group I. Surprisingly, the scotopic b-wave amplitudes in the TMP group were nearly 50% of those in Group C. The ERG examinations in the mice showed that TMP could effectively reduce the decline of the b-wave in the scotopic responses at three time points (Figure 4A). The a- and b-wave amplitudes of the mixed rod-cone responses in the TMP group declined slightly which compared with Group I at three time points; the a- and b-wave latencies were shorter than Group I at day 3 and 7 (Figure 4B). The results for the photopic responses in the mice were similar to those scotopic responses. The ERG examinations showed that TMP could effectively reduce the decline in the b-wave in the photopic responses at day 3 and 14 and the b-wave latencies of the photopic responses in the TMP group were shorter than those in Group I at three time points (Figure 4C).

TUNEL assays: TUNEL assays showed that the level of apoptosis in the retinas peaked on day 3 after $NaIO_3$ administration, then gradually decreased in the following days, and was not obvious at day 14 in Group I and the TMP group (Figure 5). TUNEL-positive cells (green) were restricted in the ONL, in which photoreceptor nuclei were located. The number of TUNEL-positive cells was statistically significantly increased in Group I compared with the TMP group at day 3 and 7 (**p<0.01; Figure 6).

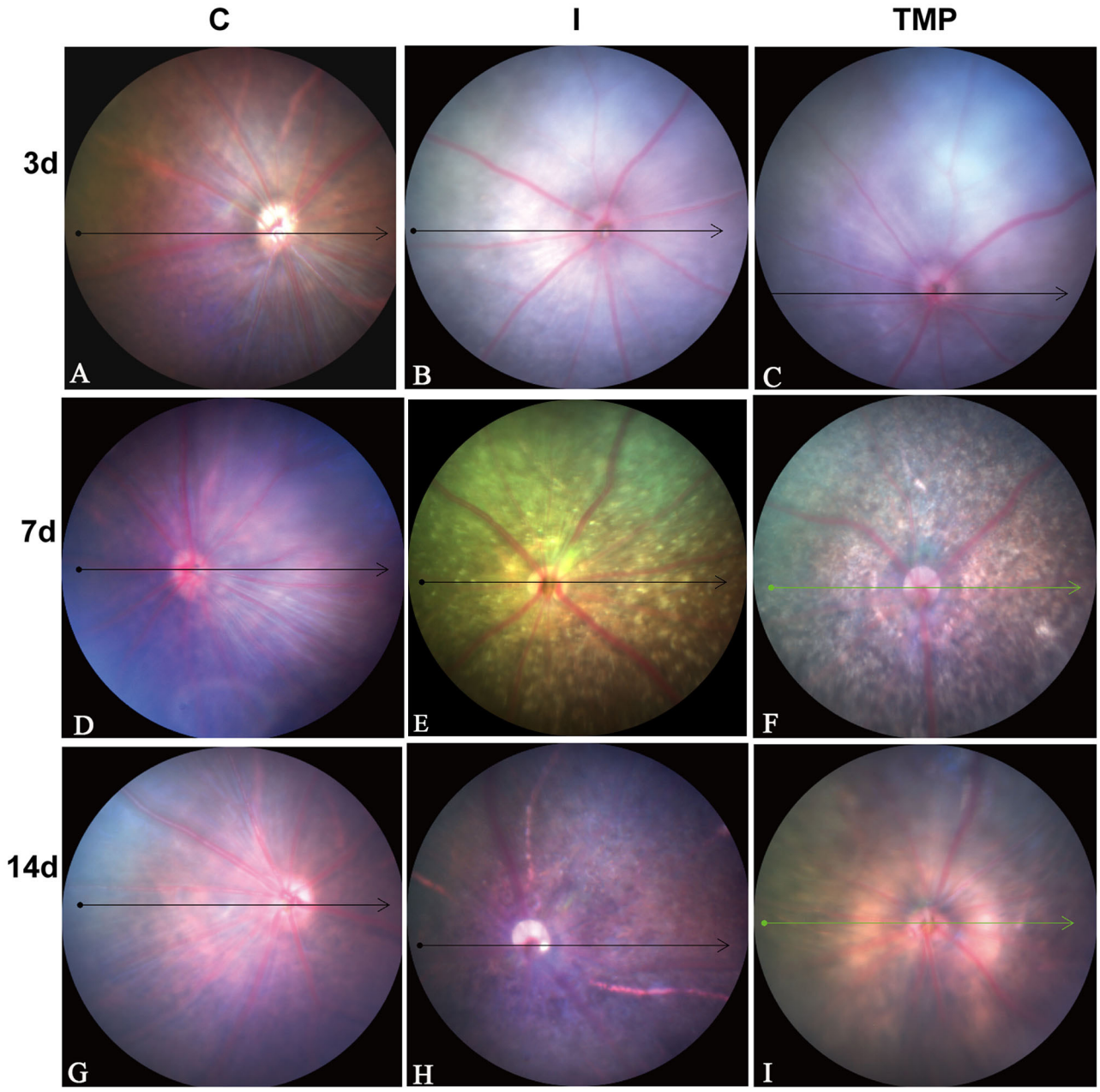

Figure 1. Color fundus photographs of mice treated with $NaIO_3$ or $NaIO_3$ + TMP at three time points. Top, middle, and bottom: three groups at day 3, 7, and 14 after the $NaIO_3$ administration. Left to right: The control group, $NaIO_3$-degenerated group (Group I), and the tetramethylpyrazine (TMP) group.

Western blotting of Nrf2, HO-1, and Bax protein expression in the retinas: Western blotting of retinal samples (n = 5) of Nrf2, HO-1 and Bax protein expression at day 3, 7, and 14 after $NaIO_3$ injection (Figure 7A). Western blotting showed that the amount of Nrf2 protein in Group I and the TMP group was statistically significantly higher than that in Group C after $NaIO_3$ injection at day 3, with a more obvious increase in the TMP group compared with that in Group I. These variations were not observed at day 14 (Figure 7B). The HO-1 levels changed with the amount of Nrf2, statistically significantly increasing at day 3 and decreasing gradually with time in Group I and the TMP group. However, there were statistically significant differences among the three groups at day 14 post-$NaIO_3$ treatment, and the TMP group showed higher amounts than Group I (Figure 7C). Western blotting also revealed that the Bax expression levels in Group

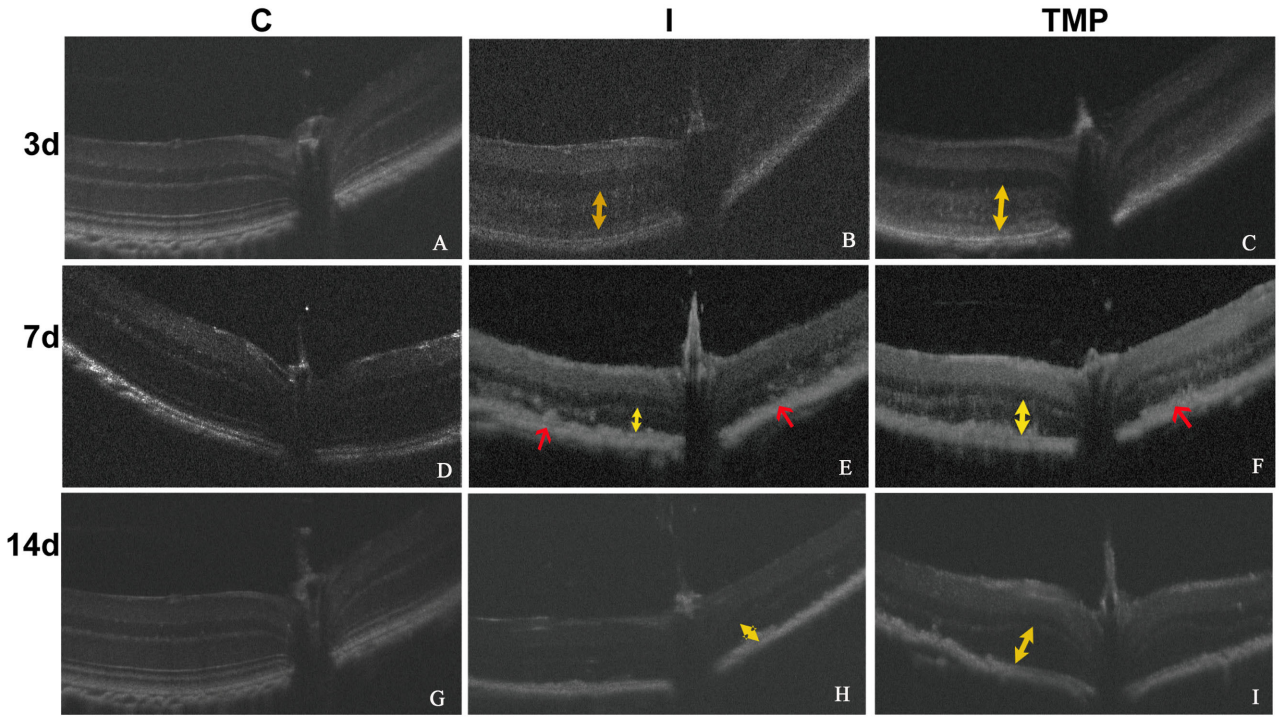

Figure 2. OCT scans of mice treated with $NaIO_3$ or $NaIO_3$ + TMP at three time points. Top, middle, and bottom: The three groups at day 3, 7, and 14 after $NaIO_3$ administration. Left to right: The control group, the $NaIO_3$-degenerated group (Group I), and the tetramethylpyrazine (TMP) group. Yellow double-headed arrows mark the outer nuclear layer (ONL) thickness. Red arrows mark the RPE migrated into the inner and outer segments (IS/OS).

I and the TMP group were much higher than those in Group C at day 3 post-$NaIO_3$ treatment. The Bax protein levels decreased gradually in the TMP group in the following days, while remaining high in Group I for 14 days. Bax expression was statistically significantly higher in Group I compared with the TMP group (Figure 7D).

DISCUSSION

AMD is the leading blinding eye diseases in individuals over 65 years old in developed countries [14]. The occurrence of dry AMD is related to oxidative stress, autophagy, inflammation, and other factors [15]. Large amounts of unsaturated fatty acids accumulate in the photoreceptor layer, which is likely to cause oxidative stress damage under continuous visible light irradiation. The retina is sensitive to oxidative stress which damages the retina aggravated by lipofuscin. We used $NaIO_3$ to make an animal model of dry AMD. TMP is an active ingredient of the traditional Chinese herbal medicine Chuanxiong. Its main pharmacological effects include antioxidative stress, antagonism for calcium, and suppression of proinflammatory factors [16]. It was reported that TMP could inhibit free radical production, had antioxidative and neuroprotective effects, and was widely used in neurologic ischemic diseases [17].

A mouse disease model similar to dry AMD was prepared by intraperitoneal injection of $NaIO_3$. In this study, we selected TMP to intervene mice retinas against $NaIO_3$-induced damage and observed morphological and functional retinal changes. Fundus photography and OCT scan showed that the mice retinas presented yellow-white deposits at day 7, accompanied by RPE layer disorder and reduction of photoreceptor cells in the ONL after $NaIO_3$ injection. H&E staining of the retinal sections showed that the retinal thickness was statistically significantly decreased after $NaIO_3$ treatment; however, the thickness of the retinal thickness in the TMP-treated group declined less than that in the $NaIO_3$-degenerated group. In conclusion, TMP could alleviate $NaIO_3$-induced retinal damage, especially protecting the ONL from injury. Retinal apoptosis peaked on day 3 after $NaIO_3$ injection, gradually decreased, and was no longer obvious on day 14. The ratios of apoptotic cells in the ONL in the $NaIO_3$-degenerated group and the TMP-treated group at day 3 and 7 were statistically significantly different. This suggested that TMP could reduce $NaIO_3$-induced apoptosis in photoreceptor

cells. Therefore, TMP could alleviate retina and ONL thickness reductions caused by $NaIO_3$.

We observed a rapid reduction in the b-wave amplitude after $NaIO_3$ treatment, in agreement with a defective synaptic transmission to the second-order neurons. The decrease in the b-wave in the TMP-treated group was nearly half that of the control group, while responses were almost disappeared in the $NaIO_3$-degenerated group. The differences were statistically significant. It was suggested that TMP could effectively protect the function of bipolar cells. The reductions in the a- and b-wave amplitudes of the mixed rod-cone responses in the TMP-treated group were less than those in the $NaIO_3$-degenerated group, suggesting that TMP can effectively protect the function of the photoreceptors. In conclusion, TMP could protect retinal function from $NaIO_3$ damage.

The Keap1-Nrf2/ARE signaling pathway confers resistance to oxidative stress due to internal or external oxidation and chemical substances, and constitutes an important protective pathway. As an antioxidative transcription factor, Nrf2 binds to the ARE antioxidant reaction and induces the expression of multiple antioxidants, anti-inflammatory proteins, and detoxifying enzymes downstream to form the Nrf2/ARE pathway. In combination with ARE, Nrf2 activates the expression of the target genes, which regulates the transcriptional activities of phase II metabolic enzymes and antioxidant enzymes, thus exerting antioxidant effects and

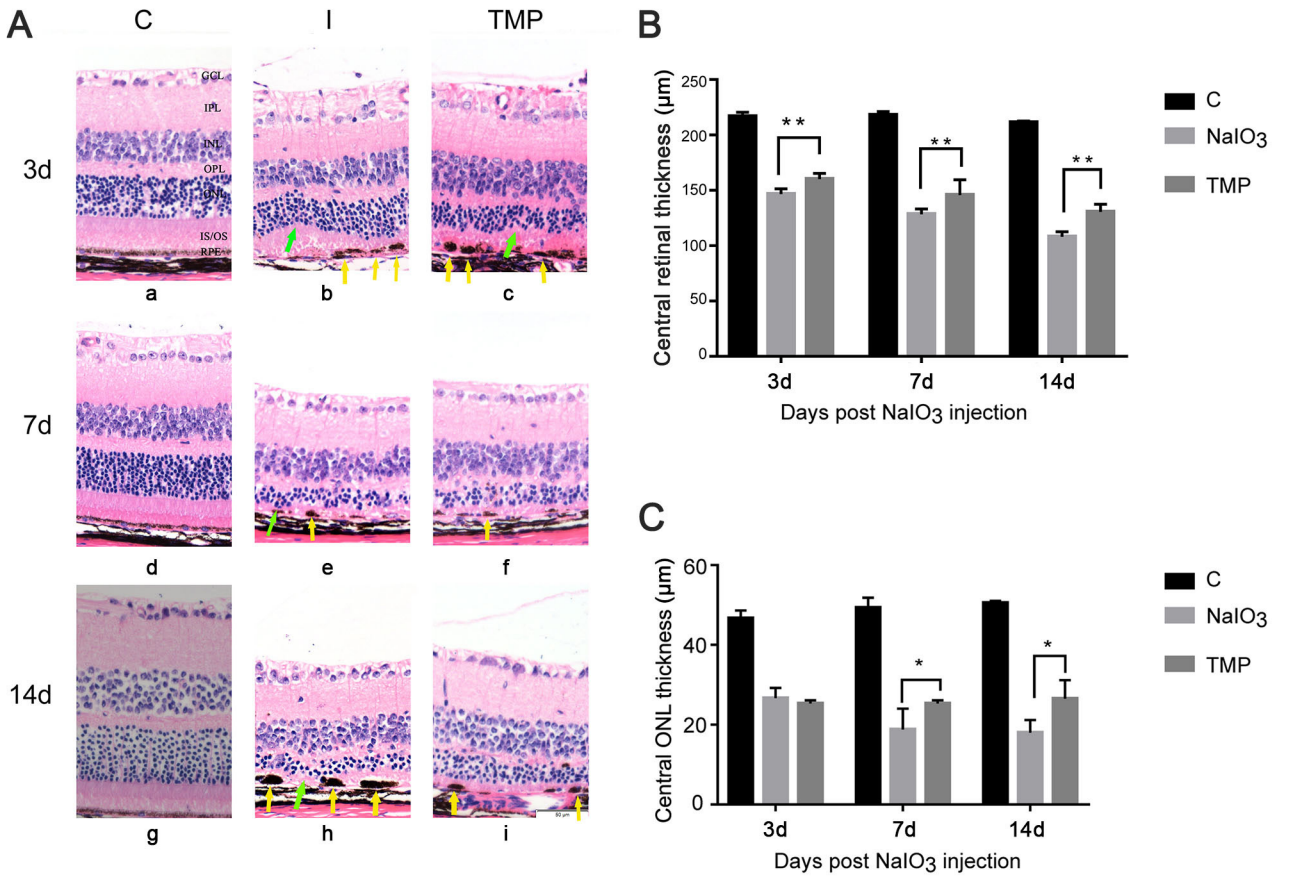

Figure 3. Altered retinal sections and thicknesses of mice treated with $NaIO_3$ or $NaIO_3$ + TMP at three time points. **A**: hematoxylin and eosin (H&E) staining of paraffin-embedded retinal cross sections of mice treated with $NaIO_3$ or $NaIO_3$ + TMP at three time points. Top, middle, and bottom: Three groups at day 3, 7, and 14 after the $NaIO_3$ administration. Left to right: The control group, the $NaIO_3$-degenerated group (Group I), and the tetramethylpyrazine (TMP) group. Green arrows mark ONLs in Group I and the TMP group were wave-like, and yellow arrows mark swelling and bundling of RPE cells migrated into the IS/OS after $NaIO_3$ administration. GCL, ganglion cell layer; IPL, inner plexiform layer; INL, inner nuclear layer; OPL, outer plexiform layer; ONL, outer nuclear layer; IS/OS, inner and outer segments. Scale bar: 50 um. **B:** Central retinal thicknesses of three groups at day 3, 7, and 14 were measured on histological sections. Asterisks indicate the statistically significant deviation of thickness between Group I and the TMP group. **C**: Central ONL thicknesses of three groups at day 3, 7, and 14 were measured on histological sections. Asterisks indicate the statistically significant deviation of thicknesses between Group I and the TMP group. (n = 5 outcomes of every mouse, **p<0.01, *p<0.05).

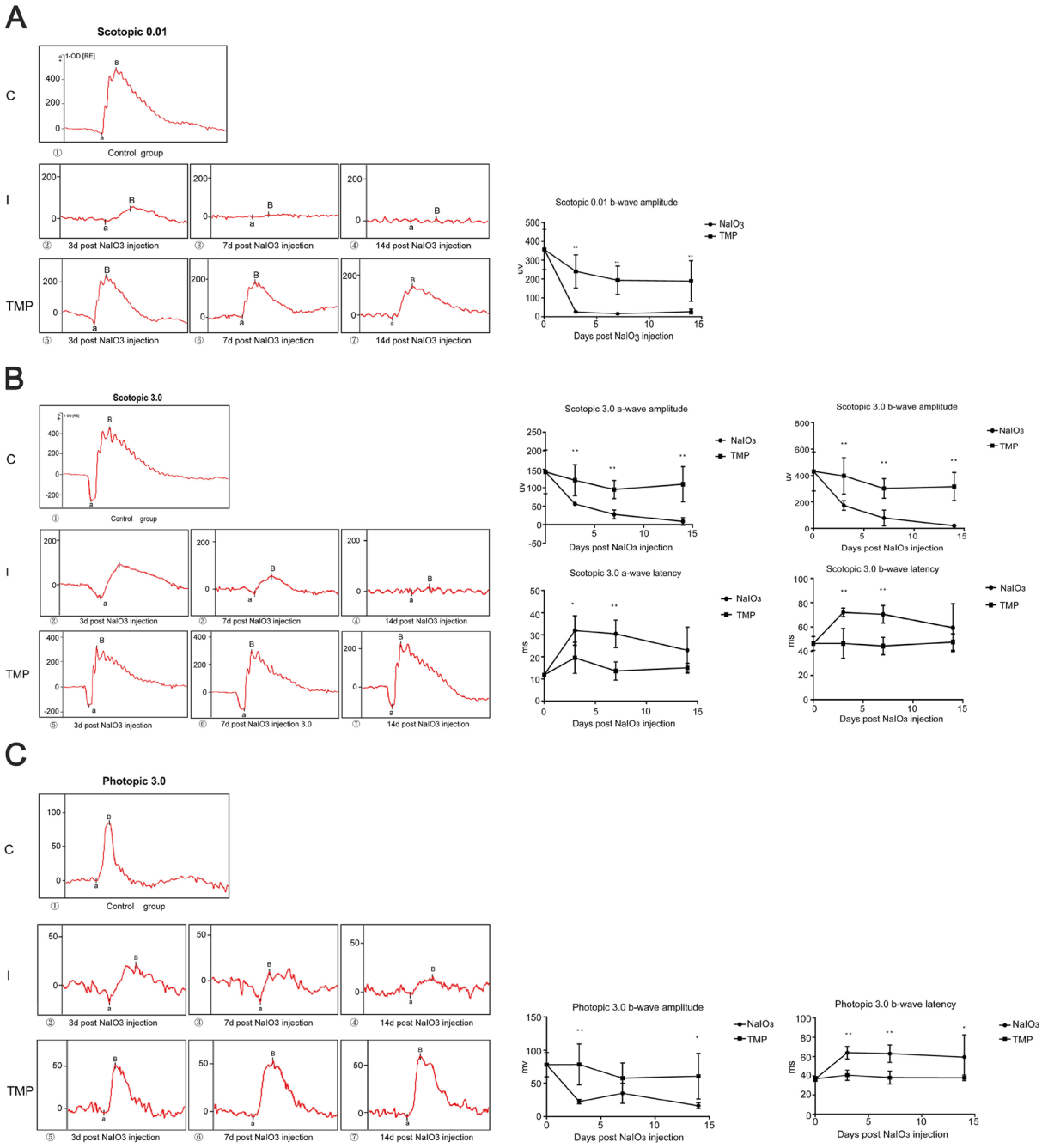

Figure 4. Analysis of retinal function of mice treated with $NaIO_3$ or $NaIO_3$ + TMP at three time points. **A**: Rod responses recorded in three groups at day 3, 7, and 14. Statistically significant reductions in the scotopic 0.01 b-wave amplitudes were observed in the $NaIO_3$-degenerated group (Group I) and the tetramethylpyrazine (TMP) group at three time points. **B**: Mixed rod-cone responses recorded in three groups at day 3, 7, and 14. The a- and b-wave amplitudes of the mixed rod-cone responses in the TMP group declined slightly compared with those in Group I at three time points. The a-wave and b-wave latencies in the TMP group were shorter than those in Group I at day 3 and 7. **C**: Cone responses recorded in the three groups at day 3, 7, and 14. Significant reductions in the photopic b-wave amplitudes were observed in Group I compared with those in the TMP group at the day 3 and 7 time points, and significant prolongations of photopic b-wave latencies were observed in Group I and the TMP group at three time points. (n = 8 retinas from 4 mice, **p<0.01, *p<0.05).

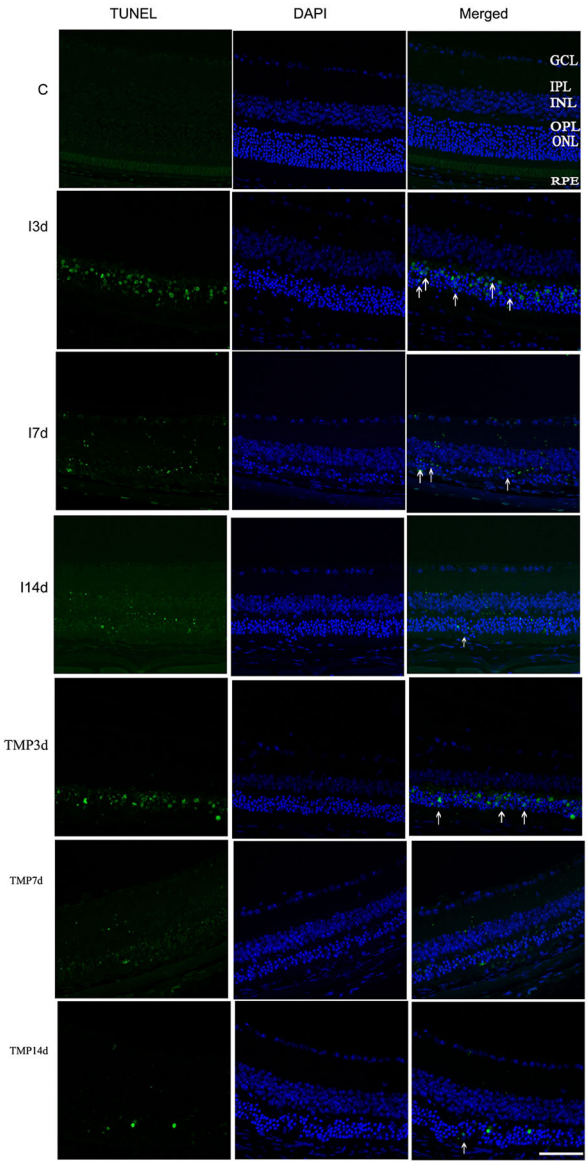

Figure 5. TUNEL assays photographs of mice treated with $NaIO_3$ or $NaIO_3$ + TMP at three points. Top: Group C. The second to fourth arrays are the $NaIO_3$-degenerated group (Group I) at day 3, 7, and 14 after $NaIO_3$ administration. The fifth to seventh arrays are the tetramethylpyrazine (TMP) group at day 3, 7, and 14 after $NaIO_3$ administration. Left to right: Terminal deoxynucleotidyl transferase dUTP nick-end labeling (TUNEL), 4′,6-diamidino-2-phenylindole (DAPI), and Merged. Group C: TUNEL-positive cells were not found in Group C. I3d: Multiple of TUNEL-positive cells (green) were found in the ONL. I7d: TUNEL-positive cells were decreased in the ONL. I14d: Few TUNEL-positive cells were found in the ONL. TMP3d: Many TUNEL-positive cells were observed in the ONL. TMP7d: TUNEL-positive cells were decreased in the ONL. TMP14d: Only a few TUNEL-positive cells were found in the ONL. White arrows mark TUNEL-positive cells. Scale bar: 50 μm.

restoring intracellular homeostasis [18]. Damage to the Nrf2 pathway leads to oxidative damage to the RPE or triggers an intrinsic immune response that induces apoptosis in RPE leading to pathological changes in AMD [19]. The impaired Nrf2 signaling pathway causes RPE oxidative damage [20]. HO-1 is a downstream product of Nrf2 activation. It not only plays a role in the body's physiologic state but also has an important function in antioxidation, antiapoptosis, and immune regulation under stress conditions.

This study showed that the amount of Nrf2 protein in the retinas after $NaIO_3$ treatment was statistically significantly higher than that in the control group. However, the increase in the TMP-treated group was more obvious at day 3 and 7. The downstream protein HO-1 changed consistently with Nrf2, and it increased statistically significantly at three time points after $NaIO_3$ treatment. Then the amount of HO-1 in two groups fell, but the amount remained higher than the control values. It indicated that treatment of $NaIO_3$ temporarily activated the expression of Nrf2 and HO-1 in the retinas against oxidation stress, and TMP could increase the expression levels. Bax is the most important apoptotic gene in the human body. It belongs to the Bcl-2 family of genes and forms a heterodimer with Bcl-2, which inhibits Bcl-2. Bax is a key component of apoptosis caused by mitochondrial stress [21]. Upon apoptotic stimulation, Bax forms oligomers and is transferred from the cytosol to the mitochondrial membrane. BAX interacts

with the voltage-dependent anion channel of the mitochondrial outer membrane to promote mitochondrial membrane permeability with transient pore opening [22]. These channels promote the release of mitochondrial membrane gap proteins and cause apoptosis. In this study, BAX amounts in retinas were statistically significantly higher than those of the control group after $NaIO_3$ injection at day 3. The amount of BAX in the TMP-treated group began to decline, but the $NaIO_3$-degenerated group retained high levels throughout 14 days. These findings indicate that treatment of $NaIO_3$ leads to BAX upregulation and causes apoptosis that peaks within 3 days, resulting in decreased retinal and ONL thicknesses and significantly impaired retinal function. Meanwhile, TMP intervention upregulates retinal Nrf2 protein and downstream HO-1, decreases BAX elevation, inhibits mitochondrial pathway activation, suppresses apoptosis, reduces retinas and ONL thinning, and decreases retinal function damage induced by $NaIO_3$. The result suggests that the protective effects of TMP against $NaIO_3$-induced injury in retinas may be mediated by upregulation of Nrf2 and HO-1 expression. Therefore, using TMP may provide a novel approach in the treatment of dry AMD.

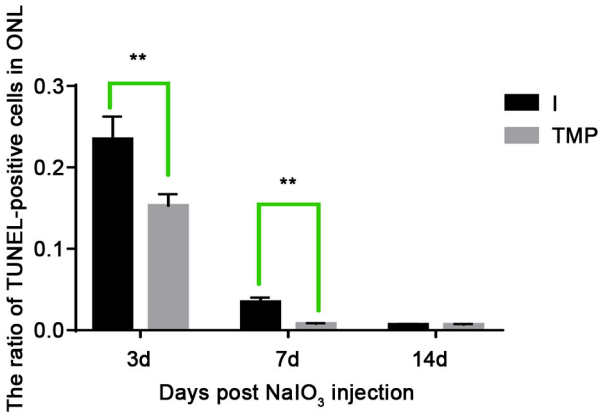

Figure 6. Statistically significant changes in the ratio of TUNEL-positive cells in the ONL between Group I and the TMP group (n = 5, **p<0.01).

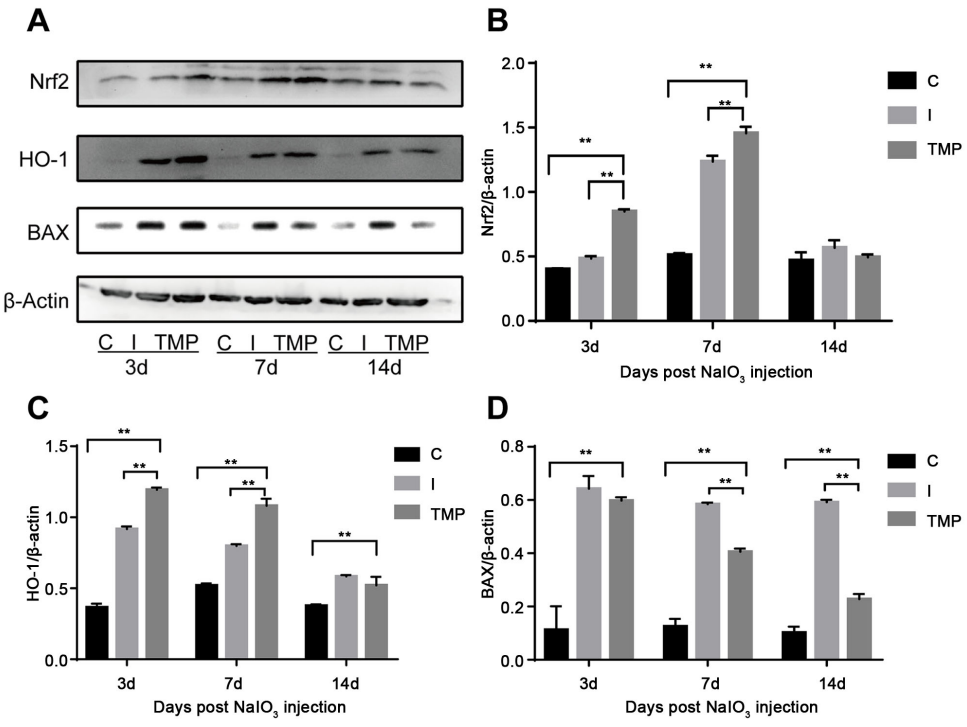

Figure 7. Western blotting analyses of expression of Nrf_2, HO-1 and Bax in retinas of mice treated with $NaIO_3$ or $NaIO_3$ + TMP at three time points. **A**: Western blot detection of Nrf2, HO-1, and BAX protein expression levels of the three groups. **B**: Nrf2 expression levels increased by approximately twofold and threefold in the tetramethylpyrazine (TMP) group at day 3 and 7 post-$NaIO_3$ injection, respectively, when compared with the control group. The increase in the TMP group was more obvious than that in the $NaIO_3$-degenerated group (Group I) at day 3 and 7 post-$NaIO_3$ injection. **C**: HO-1 expression levels were approximately twofold in the TMP group at day 3 and 7 post-$NaIO_3$ injection when compared with those of the control group. There were statistically significant differences among the three groups at the three time points, and the expression levels in the TMP group were higher than those of Group I at day 3 and 7 post-$NaIO_3$ injection. **D**: BAX expression levels increased by approximately sixfold in the TMP group and Group I at day 3 day post-$NaIO_3$ injection when compared with the control group. It decreased gradually in the TMP group in the following days but remained high in Group I for 14 days. The Bax expression levels in Group I were statistically significantly higher than those of the TMP group. (n = 3,*p<0.05, **p<0.01).

ACKNOWLEDGMENTS

This study was supported by National Nature Science Foundation of China (NO. 81,674,027), National Key R&D Program of China (2016YFC0904800) and Baoshan District Shanghai Youth Medical Talents Training Program (bswsyq2015A02), Baoshan District Ophthalmology Specialty of Integrated TCM and Western Medicine Program (BSZK2018B01).

REFERENCES

1. Resnikoff S, Pascolini D, Etya'ale D, Kocur I, Pararajasegaram R, Pokharel GP, Mariotti SP. Global data on visual impairment in the year 2002. Bull World Health Organ 2004; 82:844-51. .

2. Heier JS, Brown DM, Chong V, Korobelnik JF, Kaiser PK, Nguyen QD, Kirchhof B, Ho A, Ogura Y, Yancopoulos GD, Stahl N, Vitti R, Berliner AJ, Soo Y, Anderesi M, Groetzbach G, Sommerauer B, Sandbrink R, Simader C, Schmidt-Erfurth U. View, Groups VS. Intravitreal aflibercept (VEGF trap-eye) in wet age-related macular degeneration. Ophthalmology 2012; 119:2537-48. [PMID: 23084240].

3. Leung E, Landa G. Update on current and future novel therapies for dry age-related macular degeneration. Expert Rev Clin Pharmacol 2013; 6:565-79. [PMID: 23971874].

4. Cai X, McGinnis JF. Oxidative stress: the achilles' heel of neurodegenerative diseases of the retina. Front Biosci (Landmark Ed) 2012; 17:1976-95. [PMID: 22201850].

5. Enzmann V, Row BW, Yamauchi Y, Kheirandish L, Gozal D, Kaplan HJ, McCall MA. Behavioral and anatomical abnormalities in a sodium iodate-induced model of retinal pigment epithelium degeneration. Exp Eye Res 2006; 82:441-8. [PMID: 16171805].

6. Wang J, Iacovelli J, Spencer C, Saint-Geniez M. Direct effect of sodium iodate on neurosensory retina. Invest Ophthalmol Vis Sci 2014; 55:1941-53. [PMID: 24481259].

7. Nadal-Nicolas FM, Becerra SP. Pigment Epithelium-derived Factor Protects Retinal Pigment Epithelial Cells Against Cytotoxicity "In Vitro". Adv Exp Med Biol 2018; 1074:457-64. [PMID: 29721976].

8. Machalinska A, Lubinski W, Klos P, Kawa M, Baumert B, Penkala K, Grzegrzolka R, Karczewicz D, Wiszniewska B, Machalinski B. Sodium iodate selectively injuries the posterior pole of the retina in a dose-dependent manner: morphological and electrophysiological study. Neurochem Res 2010; 35:1819-27. [PMID: 20725778].

9. Balmer J, Zulliger R, Roberti S, Enzmann V. Retinal Cell Death Caused by Sodium Iodate Involves Multiple Caspase-Dependent and Caspase-Independent Cell-Death Pathways. Int J Mol Sci 2015; 16:15086-103. [PMID: 26151844].

10. Li WM, Liu HT, Li XY, Wu JY, Xu G, Teng YZ, Ding ST, Yu C. The effect of tetramethylpyrazine on hydrogen peroxide-induced oxidative damage in human umbilical vein endothelial cells. Basic Clin Pharmacol Toxicol 2010; 106:45-52. [PMID: 19821832].

11. Liao SL, Kao TK, Chen WY, Lin YS, Chen SY, Raung SL, Wu CW, Lu HC, Chen CJ. Tetramethylpyrazine reduces ischemic brain injury in rats. Neurosci Lett 2004; 372:40-5. [PMID: 15531085].

12. Yang Z, Zhang Q, Ge J, Tan Z. Protective effects of tetramethylpyrazine on rat retinal cell cultures. Neurochem Int 2008; 52:1176-87. [PMID: 18261827].

13. Zhu X, Wang K, Zhang K, Tan X, Wu Z, Sun S, Zhou F, Zhu L. Tetramethylpyrazine Protects Retinal Capillary Endothelial Cells (TR-iBRB2) against IL-1beta-Induced Nitrative/Oxidative Stress. Int J Mol Sci 2015; 16:21775-90. [PMID: 26370989].

14. Klein R, Cruickshanks KJ, Nash SD, Krantz EM, Nieto FJ, Huang GH, Pankow JS, Klein BE. The prevalence of age-related macular degeneration and associated risk factors. Arch Ophthalmol 2010; 128:750-8. [PMID: 20547953].

15. Bowes Rickman C, Farsiu S, Toth CA, Klingeborn M. Dry age-related macular degeneration: mechanisms, therapeutic targets, and imaging. Invest Ophthalmol Vis Sci 2013; 54:ORSF68-80. [PMID: 24335072].

16. Tan Z. Neural protection by naturopathic compounds-an example of tetramethylpyrazine from retina to brain. J Ocul Biol Dis Infor 2009; 2:57-64. [PMID: 19672463].

17. Zhang G, Zhang F, Zhang T, Gu J, Li C, Sun Y, Yu P, Zhang Z, Wang Y. Tetramethylpyrazine Nitrone Improves Neurobehavioral Functions and Confers Neuroprotection on Rats with Traumatic Brain Injury. Neurochem Res 2016; 41:2948-57. [PMID: 27452038].

18. Taguchi K, Motohashi H, Yamamoto M. Molecular mechanisms of the Keap1-Nrf2 pathway in stress response and cancer evolution. Genes Cells 2011; 16:123-40. [PMID: 21251164].

19. Handa JT. How does the macula protect itself from oxidative stress? Mol Aspects Med 2012; 33:418-35. [PMID: 22503691].

20. Sachdeva MM, Cano M, Handa JT. Nrf2 signaling is impaired in the aging RPE given an oxidative insult. Exp Eye Res 2014; 119:111-4. [PMID: 24216314].

21. Wei MC, Zong WX, Cheng EH, Lindsten T, Panoutsakopoulou V, Ross AJ, Roth KA, MacGregor GR, Thompson CB, Korsmeyer SJ. Proapoptotic BAX and BAK: a requisite gateway to mitochondrial dysfunction and death. Science 2001; 292:727-30. [PMID: 11326099].

22. Yamagata H, Shimizu S, Nishida Y, Watanabe Y, Craigen WJ, Tsujimoto Y. Requirement of voltage-dependent anion channel 2 for pro-apoptotic activity of Bax. Oncogene 2009; 28:3563-72. [PMID: 19617898].

Articles are provided courtesy of Emory University and the Zhongshan Ophthalmic Center, Sun Yat-sen University, P.R. China. The print version of this article was created on 27 June 2020. This reflects all typographical corrections and errata to the article through that date. Details of any changes may be found in the online version of the article.